

A Mets Motif Peptide Found in Copper Transport Proteins Selectively Binds Cu(I) with Methionine-Only Coordination

Jianfeng Jiang, Istvan A. Nadas, M. Alison Kim, and Katherine J. Franz*

Department of Chemistry, Duke University, P.O. Box 90346, Durham, North Carolina 27708

Received July 14, 2005

Mets motifs, which refer to methionine-rich sequences found in the high-affinity copper transporter Ctr1, also appear in other proteins involved in copper trafficking and homeostasis, including other Ctrs as well as Pco and Cop proteins isolated from copper-resistant bacteria. To understand the coordination chemistry utilized by these proteins, we studied the copper binding properties of a peptide labeled **Mets7-PcoC** with the sequence Met-Thr-Gly-Met-Lys-Gly-Met-Ser. By comparing this sequence to a series of mutants containing noncoordinating norleucine in place of methionine, we confirm that all three methionine residues are involved in a thioether-only binding site that is selective for Cu(I). Two independent methods, one based on mass spectrometry and one based on rate differences for the copper-catalyzed oxidation of ascorbic acid, provide an effective K_D of $\sim 2.5 \mu\text{M}$ at pH 4.5 for the 1:1 complex of **Mets7-PcoC** with Cu(I). These results establish that a relatively simple peptide containing an $\text{MX}_2\text{-MX}_2\text{M}$ motif is sufficient to bind Cu(I) with an affinity that corresponds well with its proposed biological function of extracellular copper acquisition.

Introduction

Copper is required by virtually all cell types from bacteria to humans as a redox-active cofactor for such critical processes as electron transport, free radical detoxification, neurotransmitter production, and others.¹ If uncontained by the appropriate biological site, however, Cu(I)/Cu(II) redox cycling can damage cells by catalyzing the production of reactive oxygen species. Cells therefore have elaborate systems for copper trafficking that ensure its safe transport along the distribution network, from extracellular acquisition to cellular uptake, delivery to end-point cuproenzymes, recycling, and clearance.²

Inside the cell, soluble chaperone proteins guide copper to the appropriate copper-dependent enzyme, as depicted in Figure 1.^{3,4} Structural studies have revealed distinct paradigms for copper binding that clearly distinguish the coordination chemistry of these trafficking proteins from that found in enzymes that utilize copper for catalytic chemistry.⁵ Mononuclear cuproenzymes provide a stable four- or five-

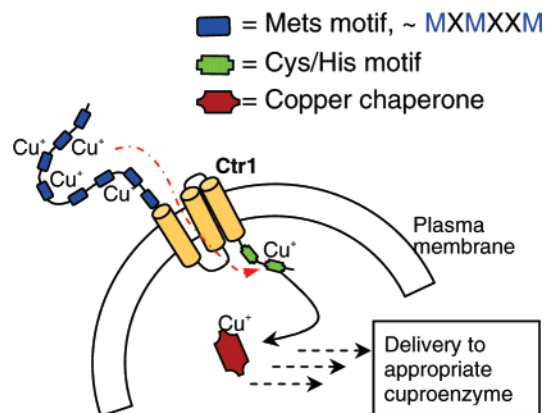


Figure 1. Schematic of cellular copper trafficking, highlighting the role of yeast Ctr1. The methionine-rich Mets motifs are suggested to bind and stabilize Cu(I).

coordinate binding site that includes histidine, cysteine, and occasionally methionine side chains. Copper chaperones, on the other hand, bind Cu(I) with cysteinate ligands in low-coordinate sites that facilitate metal-ion transfer between the chaperone and target protein. The function of these proteins therefore defines and is defined by appropriate coordination chemistry for a particular task. Understanding fundamental chemical details such as the metal oxidation state, coordination environment, geometry, and binding affinity is critical to unraveling the paradox of how cells manage a toxic yet essential cofactor.

* To whom correspondence should be addressed. E-mail: katherine.franz@duke.edu.

- (1) Peña, M. M. O.; Lee, J.; Thiele, D. J. *J. Nutr.* **1999**, 1251–1260.
- (2) Arnesano, F.; Banci, L.; Bertini, I.; Ciofi-Baffoni, S. *Eur. J. Inorg. Chem.* **2004**, 1583–1593.
- (3) Rosenzweig, A. C. *Chem. Biol.* **2002**, 9, 673–677.
- (4) O'Halloran, T. V.; Culotta, V. C. *J. Biol. Chem.* **2000**, 275, 25057–25060.
- (5) Finney, L. A.; O'Halloran, T. V. *Science* **2003**, 300, 931–936.

Table 1. Amino Acid Sequences of Yeast Ctr1 Mets Motifs

Mets #	position	M	X	X	M	X	M			
1	1–6	M	E	G	M	N	M			
2	10–15	M	N	M	D	A	M			
3	26–34	M	A	S	M	S	M	D	A	M
4	45–53	M	S	S	M	S	M	E	A	M
5	64–72	M	S	S	M	A	S	M	S	M
6	77–84	M	S	G	M	S	M	S	M	
7	102–108	M	S	G	M	S	G	M		
8	119–127	M	D	M	D	M	S	M	G	M

Whereas the chemical principles of intracellular copper trafficking are becoming well elucidated, the coordination chemistry responsible for the upstream processes of extracellular copper acquisition and transmembrane transport is still lacking. These functions are attributed to high-affinity copper transporters (Ctr), a family of integral membrane proteins that are widely conserved from yeast to humans.^{6,7} Genetic studies confirm that Ctr proteins are essential for copper acquisition, as yeast mutants lacking Ctr1 show clear signs of copper deficiency^{8,9} and mice lacking mCtr1 die in utero.^{10–12} Such studies clearly demonstrate the critical role of proper copper acquisition in mammalian development.

Ctr proteins contain three transmembrane regions that situate the amino terminus on the extracellular side with the carboxyl terminus facing the cytosol, as suggested schematically for yeast Ctr1 (yCtr1) in Figure 1.^{6,9} The protein likely exists as a homotrimer in its active form.^{7–9,13} Several conserved cysteine and histidine residues located on the cytosolic terminus have been shown to bind copper.¹⁴ The unique feature of the amino-terminal region of yCtr1, which is the first gate of entry for cellular copper, is the presence of methionine-rich domains arranged as MXXM or MXM motifs containing 3–5 methionine residues per Mets motif. Yeast yCtr1 has 8 Mets motifs, with a total of 30 methionine residues in the ~140-residue extracellular domain, whereas human hCtr1 has two Mets motifs in a 66-residue extracellular region. Serial deletions of yCtr1 Mets motifs generate strains for which growth is severely limited under low-copper conditions, suggesting that Mets motifs are essential for copper acquisition under limiting-copper conditions.⁹ The yCtr1 Mets domains are listed in Table 1.

Mets motifs have been assumed to be involved in extracellular copper acquisition ever since Ctr1 was identified as a copper transporter,^{8,9,15–17} but surprisingly little chemical

evidence exists to clarify the molecular interactions between Mets motifs and copper in Ctr proteins. Methionine has a relatively weak thioether donor group that is usually supplemented with more electron-donating thiolate or imidazolate ligands from cysteine and histidine in most currently characterized biological copper sites, although a growing number of proteins involved in copper transport are notable exceptions that utilize multiple methionines for copper binding. Examples include Pco,^{18–20} Cop,^{21–23} and CusF²⁴ proteins found in copper-resistant bacteria, as well as a newly identified bacterial copper chaperone DR1885,²⁵ and the N-terminal region of a bacterial Cu,Zn superoxide dismutase.²⁶ In most of these examples, however, histidine contributes to the coordination sphere in addition to 2–3 methionines.^{19,22,24,25}

Several lines of evidence point to Cu(I) as the active redox state for Ctr1. Metalloreductases Fre1 and Fre2 are both significant for copper acquisition in *Saccharomyces cerevisiae*,^{15,27,28} and the biological reductant ascorbate enhances copper uptake when the reductases are inactivated.²⁸ Additionally, yCtr1 is unable to transport Zn(II) or other divalent metal ions, but readily takes in Ag(I) as a surrogate for Cu(I),⁷ and the Cu(I) specific chelator bathocuproine disulfonate (BCS) severely limits copper uptake in cell culture.^{8,9} These experimental observations underscore fundamental chemical principles that are likely at play to accomplish selective, high-affinity copper acquisition and transport: reduced Cu(I) will be more kinetically labile than Cu(II), and a soft, thio-rich environment should favor coordination to the soft Cu(I) and stabilize this low oxidation state in an oxidizing environment. From the point of view of coordination chemistry, the Mets motifs appear ideally suited for their proposed function.

To test this hypothesis, we chose to use synthetic peptides to identify the minimal copper-binding motif that could be functionally relevant to Ctr1. Synthetic peptides have proven to be valuable models for understanding the structure and

- (6) Puig, S.; Thiele, D. J. *Curr. Opin. Chem. Biol.* **2002**, *6*, 171–180.
 (7) Lee, J.; Peña, M. M. O.; Nose, Y.; Thiele, D. J. *J. Biol. Chem.* **2002**, *277*, 4380–4387.
 (8) Dancis, A.; Haile, D.; Yuan, D. S.; Klausner, R. D. *J. Biol. Chem.* **1994**, *269*, 25660–25667.
 (9) Puig, S.; Lee, J.; Lau, M.; Thiele, D. J. *J. Biol. Chem.* **2002**, *277*, 26021–26030.
 (10) Lee, J.; Prohaska, J. R.; Thiele, D. J. *Proc. Natl. Acad. Sci. U.S.A.* **2001**, *98*, 6842–6847.
 (11) Kuo, Y.-M.; Zhou, B.; Cosco, D.; Gitschier, J. *Proc. Natl. Acad. Sci. U.S.A.* **2001**, *98*, 6836–6841.
 (12) Lee, J.; Petris, M. J.; Thiele, D. J. *J. Biol. Chem.* **2002**, *277*, 40253–40259.
 (13) Aller, S. G.; Eng, E. T.; De Feo, C. J.; Unger, V. M. *J. Biol. Chem.* **2004**, *279*, 53435–53441.
 (14) Xiao, Z.; Loughlin, F.; George, G. N.; Howlett, G. J.; Wedd, A. G. *J. Am. Chem. Soc.* **2004**, *126*, 3081–3090.
 (15) Dancis, A.; Yuan, D. S.; Haile, D.; Askwith, C.; Eide, D.; Moehle, C.; Kaplan, J.; Klausner, R. D. *Cell* **1994**, *76*, 393–402.

- (16) Guo, Y.; Smith, K.; Lee, J.; Thiele, D. J.; Petris, M. J. *J. Biol. Chem.* **2004**, *279*, 17428–17433.
 (17) Eisses, J. F.; Chi, Y.; Kaplan, J. H. *J. Biol. Chem.* **2005**, *280*, 9635–9639.
 (18) Lee, S. M.; Grass, G.; Rensing, C.; Barrett, S. R.; Yates, C. J. D.; Stoyanov, J. V.; Brown, N. L. *Biochem. Biophys. Res. Commun.* **2002**, *295*, 616–620.
 (19) Peariso, K.; Huffman, D. L.; Penner-Hahn, J. E.; O'Halloran, T. V. *J. Am. Chem. Soc.* **2003**, *125*, 342–343.
 (20) Wernimont, A. K.; Huffman, D. L.; Finney, L. A.; Demeler, B.; O'Halloran, T. V.; Rosenzweig, A. C. *J. Biol. Inorg. Chem.* **2003**, *8*, 185–194.
 (21) Cha, J.-S.; Cooksey, D. A. *Proc. Natl. Acad. Sci. U.S.A.* **1991**, *88*, 8915–8919.
 (22) Arnesano, F.; Banci, L.; Bertini, I.; Mangani, S.; Thompsett, A. R. *Proc. Natl. Acad. Sci. U.S.A.* **2003**, *100*, 3814–3819.
 (23) Koay, M.; Zhang, L.; Yang, B.; Maher, M. J.; Xiao, Z.; Wedd, A. G. *Inorg. Chem.* **2005**, *44*, 5203–5205.
 (24) Loftin, I. R.; Franke, S.; Roberts, S. A.; Weichsel, A.; Héroux, A.; Montfort, W. R.; Rensing, C.; McEvoy, M. M. *Biochemistry* **2005**, *44*, 10533–10540.
 (25) Banci, L.; Bertini, I.; Ciofi-Baffoni, S.; Katsari, E.; Katsaros, N.; Kubicek, K.; Mangani, S. *Proc. Natl. Acad. Sci. U.S.A.* **2005**, *102*, 3994–3999.
 (26) D'Angelo, P.; Pacello, F.; Mancini, G.; Proux, O.; Hazemann, J. L.; Desideri, A.; Battistoni, A. *Biochemistry* **2005**, *44*, 13144–13150.
 (27) Georgatsou, E.; Mavrogiannis, L. A.; Fragiadakis, G. S.; Alexandraki, D. *J. Biol. Chem.* **1997**, *272*, 13786–13792.
 (28) Hassett, R.; Kosman, D. J. *J. Biol. Chem.* **1995**, *270*, 128–134.

function of metalloproteins,^{29,30} particularly binding sites for soft metal ions such as Pb(II),³¹ Hg(II),^{32,33} Cd(II),³⁴ and both Cu(I) and Cu(II).^{35–38} In this report, we investigate the coordination properties and conditional binding affinities of synthetic Mets peptides for copper. The results show that a methionine-only binding site with three methionines is sufficient for binding and stabilizing Cu(I). This all-methionine coordination motif represents an emerging paradigm for bioinorganic copper.

Experimental Section

Peptide Synthesis and Purification. Mets7-PcoC and mutants N1, N2, N3, and N4 were synthesized on a Protein Technologies PS3 automated peptide synthesizer on PAL-PEG-PS resin (Applied Biosystems) in 0.05 mmol scales. Couplings of standard Fmoc (9-fluorenylmethoxy-carbonyl)-protected amino acids (Chem-Impex) were achieved with HBTU (*O*-benzotriazole-*N,N,N',N'*-tetramethyluronium hexafluorophosphate; Novabiochem) in the presence of *N*-methylmorpholine (NMM) in *N,N'*-dimethylformamide (DMF) for 20 min cycles. Fmoc deprotection was achieved with 20% piperidine in DMF. The N-termini of all peptides were acetylated with acetic anhydride and NMM. Side-chain deprotection and peptide cleavage from the resin were achieved by treating the resin-bound peptides with a 5 mL cocktail of 95% trifluoroacetic acid (TFA), 2.5% ethane dithiol (EDT), and 2.5% triisopropylsilane (TIS) for 2–4 h under N₂. An additional 75 μL of EDT and 65 μL of bromotrimethylsilane (TMSBr) were added during the final 30 min to minimize methionine oxidation. After evaporation of TFA under N₂, the peptides were washed three times with cold diethyl ether, air-dried, and purified by semipreparative reversed-phase HPLC on a YMC C18 column with a linear 40-min gradient from 7 to 70% acetonitrile in water with 0.1% TFA. The purity was validated to be >95% by analytical HPLC, and the mass of each peptide was confirmed by ESI-MS. **Mets7-PcoC** calcd for C₃₄H₆₂N₁₀O₁₁S₃: 882.38. Found: (M + H⁺) 883.30. **N1, N2, N3** calcd for C₃₅H₆₄N₁₀O₁₁S₂: 864.42. Found: (M + H⁺) 865.30. **N4** calcd for C₃₆H₆₆N₁₀O₁₁S: 846.46. Found: (M + H⁺) 847.40.

Preparation of Stock Solutions. Stock solutions of peptides were prepared by adding 4–8 mg of purified, lyophilized peptide to a pretared vial containing 0.5 mL of Nanopure water. This procedure eliminated weighing errors associated with static electricity. Concentration was verified by quantitative amino acid analysis (Dana Farber Cancer Institute). Stock peptide solutions were periodically checked by HPLC to verify that they remained in the reduced state; they were stable to oxidation in aqueous solution at room temperature for several days. For storage, samples were kept at –20 °C in powder form or frozen aqueous solution. Copper stock

solutions were prepared in Nanopure water from CuSO₄·5H₂O (Sigma), and were standardized by EDTA titration in ammonia solution with a murexide indicator.³⁹ Ascorbic acid stock solutions were prepared fresh⁴⁰ from L-(+)-ascorbic acid (Acros 99%) in Nanopure water.

Mass Spectrometry. Electrospray ionization mass spectrometry (ESI-MS) was performed with an electrospray quadrupole ion trap mass spectrometer (1100 Series LC/MSD Trap, Agilent, Palo Alto, CA) with a conversion dynode detector (Daly). Samples were infused via a Harvard Apparatus (Holliston, MA) syringe pump at 33 μL/min. Ionization was achieved in the positive ion mode by application of +5 kV at the entrance to the capillary; the pressure of the nebulizer gas was 20 psi. The drying gas was heated to 325 °C at a flow of 7 L/min. Full-scan mass spectra were recorded in the mass/charge (*m/z*) range of 200–2000.

UV–Visible Spectroscopy. Absorption spectra were recorded in 1-cm quartz cuvettes on an SI Photonics (Tucson, AZ) model 420 fiber optic CCD array UV–vis spectrophotometer. In a typical experiment, the ascorbic acid absorbance at 255 nm of a mixture of 120 μM ascorbic acid, 8 μM CuSO₄, and 0.4–200 μM peptide was recorded every 5 s for 100 s. This time frame is only the initial portion of the first-order decay curve, which is exponential over three half-lives (*A*₂₅₅ = 1.6–0.2). Ascorbic acid solutions were adjusted to pH 4.5 with NaOH, and the pH was remeasured after the oxidation reactions to verify that the pH remained constant. Reactions were run at ambient room temperature, which was determined to be 23 °C.

Iron-catalyzed reactions were carried out in 120 μM ascorbic acid, 0.1 M KNO₃, and 8 μM Fe(NO₃)₃. The pH was adjusted to 1.75 by the addition of 1 N HCl. The low pH was required to avoid hydrolysis of Fe(III). Under these conditions, the oxidation rate of ascorbic acid was linear between 1 and 15 μM Fe(NO₃)₃.

Calculation of the Effective Dissociation Constant (*K*_D). *K*_D in these experiments is the effective dissociative binding constant of copper ion with peptide in the reducing environment of ascorbic acid (H₂Asc). Assuming a 1:1 binding stoichiometry described by eq 1, the expression for *K*_D is described by eq 2

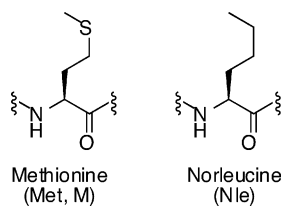


$$K_D = \frac{[P][Cu]}{[PCu]} \quad (2)$$

where [PCu] represents the amount of peptide–copper complex, [P] is the concentration of free peptide, and [Cu] is the concentration of free copper in an unspecified oxidation state. Buffers were excluded to avoid possible Cu–buffer interactions, and these expressions ignore the presence of possible Cu–ascorbate complexes. Metal complexes of ascorbate and dehydroascorbate are quite weak, and would represent very minor species in these reaction mixtures.⁴¹ Equation 3 defines the rate expression for the Cu-catalyzed ascorbate oxidation,⁴² and eq 4 defines *k*_{obs}; combining these expressions provides the first-order expression in eq 5. The slope of the line of ln[HAsc[–]] (from *A*₂₅₅ measurements) vs time therefore provides the value for *k*_{obs}. Under our working copper concentrations between 1 and 16 μM CuSO₄, plots of *k*_{obs} vs [Cu] are linear and thus provide a standard curve to obtain values of

- (29) Ghosh, D.; Pecoraro, V. L. *Inorg. Chem.* **2004**, *43*, 7902–7915.
 (30) Xing, G.; DeRose, V. J. *Curr. Opin. Chem. Biol.* **2001**, *5*, 196–200.
 (31) Payne, J. C.; ter Horst, M. A.; Godwin, H. A. *J. Am. Chem. Soc.* **1999**, *121*, 6850–6855.
 (32) Ghosh, D.; Lee, K.-H.; Demeler, B.; Pecoraro, V. L. *Biochemistry* **2005**, *44*, 10732–10740.
 (33) Veglia, G.; Porcelli, F.; DeSilva, T.; Prantner, A.; Opella, S. J. *J. Am. Chem. Soc.* **2000**, *122*, 2389–2390.
 (34) Kharenko, O. A.; Ogawa, M. Y. *J. Inorg. Biochem.* **2004**, *98*, 1971–1974.
 (35) Daugherty, R. G.; Wasowicz, T.; Gibney, B. R.; DeRose, V. J. *Inorg. Chem.* **2002**, *41*, 2623–2632.
 (36) Myari, A.; Hadjiliadis, N.; Fatemi, N.; Sarkar, B. *J. Inorg. Biochem.* **2004**, *98*, 1483–1494.
 (37) Schnepf, R.; Haehnel, W.; Wieghardt, K.; Hildebrandt, P. *J. Am. Chem. Soc.* **2004**, *126*, 14389–14399.
 (38) Sénéque, O.; Crouzy, S.; Boturyn, D.; Dumy, P.; Ferrand, M.; Delangle, P. *Chem. Commun.* **2004**, 770–771.

- (39) Flaschka, H. A. *EDTA Titrations: An Introduction to Theory and Practice*; Pergamon Press: New York, 1959.
 (40) Buettner, G. R.; Jurkiewicz, B. A. *Radiat. Res.* **1996**, *145*, 532–541.
 (41) Martell, A. E. *Ascorbic Acid: Chemistry, Metabolism, and Uses*; Advances in Chemistry Series, Vol. 200; American Chemical Society: Washington, DC, 1982; pp 153–178.
 (42) Khan, M. M. T.; Martell, A. E. *J. Am. Chem. Soc.* **1967**, *89*, 4176–4185.

Table 2. Amino Acid Sequences of Model Peptides^a

Mets7-PcoC	M	T	G	M	K	G	M	S
N1	Nle	T	G	M	K	G	M	S
N2	M	T	G	Nle	K	G	M	S
N3	M	T	G	M	K	G	Nle	S
N4	Nle	T	G	M	K	G	Nle	S

^aAll peptides contain an N-terminal acetyl cap and have C-terminal amides.

[Cu] from k_{obs} values measured in the presence of peptide.

$$\frac{-d[\text{HAsc}^-]}{dt} = k[\text{HAsc}^-][\text{Cu}^{2+}] \quad (3)$$

$$k_{\text{obs}} = k[\text{Cu}^{2+}] \quad (4)$$

$$\frac{-d[\text{HAsc}^-]}{dt} = k_{\text{obs}}[\text{HAsc}^-] \quad (5)$$

The remaining quantities [P] and [PCu] in the K_D expression of eq 2 are defined by eqs 6 and 7, where [Cu]_T and [P]_T are the known total concentrations of copper and peptide, respectively, adjusted for dilution when necessary.

$$[\text{PCu}] = [\text{Cu}]_{\text{T}} - [\text{Cu}] \quad (6)$$

$$[\text{P}] = [\text{P}]_{\text{T}} - [\text{PCu}] \quad (7)$$

For the case of **Mets7-PcoC**, each measurement was done on independently prepared samples. The K_D value of 2.5 ± 0.5 represents the average from six measurements taken at [P]_T between 5 and 20 μM . The higher concentrations of peptide needed in the cases of the mutant peptides necessitated that samples be made by continuous addition of the peptide stock solution. Additional H_2Asc was added periodically to restore the A_{255} level in these cases.

Equation 2 was also used to calculate K_D values from mass spectrometry data. Values for free, apo-peptide [P] were obtained by comparing the intensity of the $\text{M} + \text{H}^+$ signal to a standard curve generated for each peptide. Plots of signal intensity vs peptide concentration are linear for all five peptides in the 0–25 μM concentration range studied. All standards and samples contained 5 mM H_2Asc at pH 3.5. Samples were prepared with 20 μM peptide and CuSO_4 from 0 to 200 μM . [PCu] was calculated from eq 7, and free [Cu] from eq 6. The K_D values listed in Table 3 are each the average of five spectra taken at varying [P]_T: [Cu]_T ratios.

Results

Initial efforts to study synthetic peptides corresponding to sequences of Mets1 and Mets2 were hampered by poor water solubility, and thus we chose a sequence that includes a positively charged lysine for improved solubility. The $\text{MX}_2\text{-MX}_2\text{M}$ motif Met-Thr-Gly-Met-Lys-Gly-Met-Ser derives from residues 41–48 of PcoC, an *Escherichia coli* copper resistance protein.²⁰ It is designated **Mets7-PcoC** throughout this paper, as it is most similar to yCtr1's Mets7, which has Ser residues in place of Thr and Lys. Aqueous solutions of

Mets7-PcoC reach concentrations up to 60 mM, or greater than 50 mg/mL. For these studies, we synthesized a series of peptides in which one or two methionines are replaced with norleucine, a non-sulfur analogue. The sequences of the mutant peptides, labeled **N1–N4**, are listed in Table 2.

The peptides were synthesized by standard Fmoc solid-phase peptide synthesis, and peptide cleavage conditions were optimized to minimize methionine oxidation, which is readily detected by a shift in retention time on HPLC.

We have developed two methods to elucidate the binding motif and binding ability of **Mets7-PcoC** peptides, one based on mass spectrometry and the other a UV–vis assay. Both methods rely on ascorbic acid (H_2Asc) as a biologically relevant reductant to convert Cu(II) to Cu(I) .

Analysis of Peptide–Copper Binding by Mass Spectrometry. Figure 2 shows a series of electrospray mass spectra of 20 μM samples of peptides in the absence or presence of equimolar CuSO_4 and 5 mM H_2Asc . The singly charged ion is the most intense signal for all of the apo-peptides, as shown by the strong $\text{M} + \text{H}^+$ peak in Figure 2a at $m/z = 883.30$ for **Mets7-PcoC**. The intensity of this peak is unchanged when Cu(II) is added, as shown in Figure 2b. A peptide– Cu(II) adduct would be expected at $m/z = 472.66$ for its doubly charged ion $[\text{M} + \text{Cu(II)}]/2$, but no such peak is observed in Figure 2b or in spectra taken with more than 5-fold excess copper (data not shown). Likewise, no peak has been observed at $m/z \approx 315$, which would correspond to $[\text{M} + \text{Cu(II)} + \text{H}^+]/3$. The retention of the apo-peptide signal intensity combined with the absence of new peaks confirms that **Mets7-PcoC** has little if any affinity for Cu(II) . Upon the addition of excess H_2Asc , however, the $\text{M} + \text{H}^+$ signal at $m/z = 883.30$ decreases, whereas a new signal at 473.10 emerges and intensifies at the expense of the apo-peptide signal at higher Cu:peptide ratios (data not shown). This peak matches the calculated value of 473.16 for $[\text{M} + \text{Cu(I)} + \text{H}^+]/2$. The difference of one mass unit between the calculated values of the doubly charged ion for the peptide plus Cu(I) plus a proton vs peptide plus Cu(II) is sufficient to characterize this signal unequivocally as the result of a 1:1 complex between **Mets7-PcoC** and Cu(I) .

Replacing just one methionine residue of **Mets7-PcoC** with norleucine diminishes the ability of **N1**, **N2**, and **N3** to bind Cu(I) . Panels d, e, and f of Figure 2 show the spectra for **N1**, **N2**, and **N3**, respectively, in the presence of both CuSO_4 and H_2Asc . These three mutants show some binding to Cu(I) at $m/z = 464.10$, which matches the calculated value of 464.18 for $[\text{M} + \text{Cu(I)} + \text{H}^+]/2$. However, the ratio of apo-peptide to peptide– Cu (PCu) is higher for the mutants compared with the parent **Mets7-PcoC**. Furthermore, mutants **N1** and **N3**, in which either the N-terminal or C-terminal methionine is replaced by norleucine, are slightly better at binding Cu(I) than mutant **N2**, which lacks the middle methionine. This comparison suggests that the thioether donors are more effective chelating ligands if they are separated by no more than two intervening amino acids. When only one methionine residue is present, as is the case with **N4**, the Cu(I) binding ability is even more severely restricted. No PCu peak is found in Figure 2g, and only a

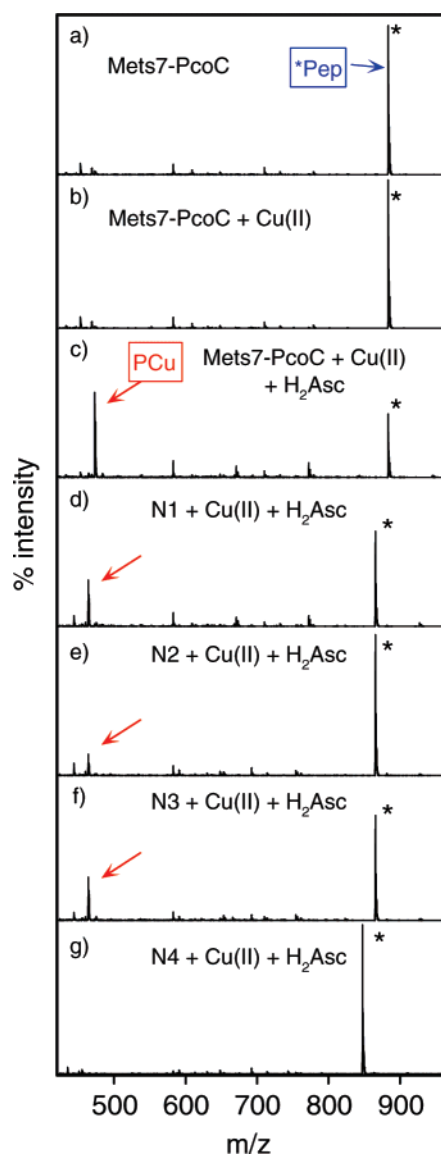


Figure 2. ESI-MS(+) of peptides and their Cu(I) adducts. Apopeptides occur at $z = 1$, and are denoted by asterisks (*); Cu adducts appear at $z = 2$ for $[\text{pep} + \text{Cu}(\text{I}) + \text{H}^+]/2$, and are marked by arrows. (a) **Mets7-PcoC** showing $\text{M} + \text{H}^+$ at m/z 883.30. (b) Adding Cu(II) causes no change from (a), indicating no binding. (c) Adding H_2Asc to the sample in (b) reduces Cu(II) to Cu(I), which forms an adduct with **Mets7-PcoC** at m/z 473.10. (d–g) **N1**, **N2**, **N3**, and **N4**, respectively, in the presence of H_2Asc and CuSO_4 . No Cu adduct is detected for **N4**. Samples contain $20 \mu\text{M}$ peptide, and where indicated include $20 \mu\text{M}$ CuSO_4 and 5 mM H_2Asc at pH 3.5.

weak signal for this species is detectable at P:Cu ratios up to 1:5 (data not shown).

These results clearly demonstrate the capability of a specific, methionine-rich peptide to bind Cu(I). Removing even one methionine negates this function and establishes the $\text{MX}_2\text{MX}_2\text{M}$ motif as a Cu(I) binding domain. Consistent with this Cu(I) selectivity is the fact that we observe peptide–metal species by mass spectrometry for soft, monovalent Ag(I), which is a reasonable surrogate for Cu(I) that does not require a reductant, but not for Zn(II) (data not shown).

A more quantitative analysis of the binding affinity of these peptides for Cu(I) was obtained by comparing the signal intensities for the apopeptide peak of samples containing copper and H_2Asc to a standard curve of the free peptide.

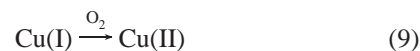
Table 3. Effective K_D Values Obtained from Mass Spectrometry for 1:1 Peptide–Cu(I) Complexes

peptide	effective K_D (μM) ^a
Mets7-PcoC	2.6 ± 0.7
N1	20 ± 9
N2	45 ± 20
N3	16 ± 7
N4	90 ± 20

^a In 5 mM H_2Asc , pH 3.5.

Because ionization efficiencies can differ significantly for different charge states and different adducts, the signal intensity corresponding to PCu is unreliable for directly calculating its concentration. Instead, we make a reasonable assumption that the amount of lost apopeptide signal corresponds to the amount of PCu formed. By using this method, $[\text{Cu}]_{\text{free}}$, $[\text{P}]_{\text{free}}$, and $[\text{PCu}]$ are readily obtained to calculate effective K_D values, which are listed in Table 3. The $2.6(7) \mu\text{M}$ dissociation constant obtained by this method for **Mets7-PcoC** is more than an order of magnitude tighter than that for mutants **N1** and **N3**; **N2** and especially **N4** have the weakest affinity for Cu(I).

Analysis of Peptide–Copper Binding by the Oxidation Rate of Ascorbate. Ascorbic acid is stable to aerial oxidation in the absence of metal ions, but copper or iron ions catalyze its oxidative degradation via eqs 8 and 9.⁴¹ The loss of its characteristic, pH-dependent absorption band between 245 and 265 nm is therefore a convenient spectroscopic signal for the presence of catalytic metal ions.^{40,43,44}



The pH-dependent oxidation rate is first-order with respect to both the ascorbate monoanion (HAsc^-) and the metal ion,⁴² and is known to decrease in the presence of metal chelators, with slower oxidation rates corresponding to more stable chelates.^{44,45} Chelators that favor the high-valence oxidation state slow the rate by making eq 8 rate-limiting, whereas molecules that stabilize Cu(I) shift the rate-limiting step to eq 9, as has been shown for ascorbate oxidation in aqueous acetonitrile.⁴⁶ The ascorbate UV–vis assay described here provides a convenient spectroscopic signal for monitoring the binding ability of the Mets peptides with spectroscopically silent Cu(I).

We examined the effects of the Mets peptides on Cu-catalyzed ascorbic acid oxidation by monitoring the loss of absorbance at 255 nm of $120 \mu\text{M}$ H_2Asc at pH 4.5. This pH is optimal for these studies for several reasons. Because the oxidation rate increases with increased concentration of HAsc^- , which has a $\text{p}K_a$ of 4.1, running the reaction at elevated pH values amplifies unwanted errors. In addition, the hydrolysis of Cu(II) is minimal at this pH. Most importantly, yeast cells expressing Ctr1 acidify their media to pH 4–5, and hCtr1-transfected human cells increase Cu

(43) Buettner, G. R. *J. Biochem. Biophys. Methods* **1988**, *16*, 27–40.

(44) Buettner, G. R. *Free Radical Res. Commun.* **1986**, *1*, 349–353.

(45) Khan, M. M. T.; Martell, A. E. *J. Am. Chem. Soc.* **1967**, *89*, 7104–7111.

(46) Mi, L.; Zuberbühler, A. D. *Helv. Chim. Acta* **1992**, *75*, 1547–1556.

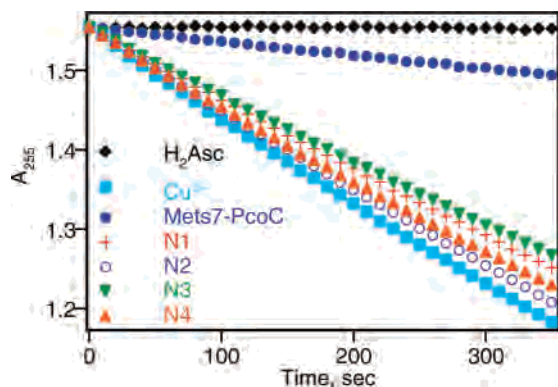


Figure 3. Solutions of $120\ \mu\text{M}$ H_2Asc at pH 4.5 do not autoxidize in air, as shown by the stability of A_{255} (black diamonds). Addition of $8\ \mu\text{M}$ CuSO_4 catalyzes ascorbate oxidation, as shown by the loss of A_{255} (blue squares). **Mets7-PcoC** ($20\ \mu\text{M}$) significantly prevents Cu-catalyzed ascorbate oxidation (solid blue circles), but even $100\ \mu\text{M}$ solutions of mutant peptides **N1–N4** are not capable of preventing oxidation (remaining symbols).

uptake at low extracellular pH.⁷ Therefore, pH 4.5 represents a biologically relevant pH for these peptides.

The black diamonds in Figure 3 show the control reaction of freshly prepared H_2Asc in the absence of added metal or peptide. The persistence of the absorbance at 255 nm over time demonstrates the stability of the ascorbic acid solution. Upon addition of $8\ \mu\text{M}$ CuSO_4 , the A_{255} signal steadily decays (blue squares), indicating catalytic ascorbate oxidation. This catalytic cycle, however, is severely inhibited by the addition of $20\ \mu\text{M}$ **Mets7-PcoC**, as demonstrated by the solid blue circles in Figure 3 that show only a slight decrease over time, suggesting that **Mets7-PcoC** is chelating Cu(I) and preventing its participation in the redox cycle. Although this experiment alone does not prove which copper oxidation state the peptide prefers, the previously described mass spectral evidence convincingly suggests it is Cu(I).

The remaining plots of Figure 3 show the trend of the A_{255} signal in the presence of $8\ \mu\text{M}$ CuSO_4 and $100\ \mu\text{M}$ solutions of each of the mutant peptides. Although these peptides differ by only the replacement of 1 or 2 thioether-containing residues, none significantly attenuates the ascorbate oxidation rate. Replacing even one of the methionine residues with a nondonating group abrogates the ability of these peptides to stabilize copper. Taken together, the data in Figure 3 demonstrate that the $\text{MX}_2\text{MX}_2\text{M}$ motif of **Mets7-PcoC** is ideally suited for sequestering Cu(I).

To assess the effective binding affinity of these peptides for Cu, we studied the Cu-catalyzed ascorbate oxidation rate as a function of peptide concentration and compared the observed rate constant (k_{obs}) to a standard curve of k_{obs} vs $[\text{Cu}]$. The standard curve in Figure 4 demonstrates that k_{obs} is directly proportional to the concentration of available (unchelated) copper in solution, and thereby provides an estimation of the catalytically active Cu present for a specific value of k_{obs} obtained from the experiments with added peptide. Plots of k_{obs} vs $[\text{peptide}]$ are shown in Figure 5 for **Mets7-PcoC** and the mutants **N1–N4**.

Two significant differences between these plots should be addressed. The first is the order of magnitude difference in scale for the concentration of peptide needed to significantly

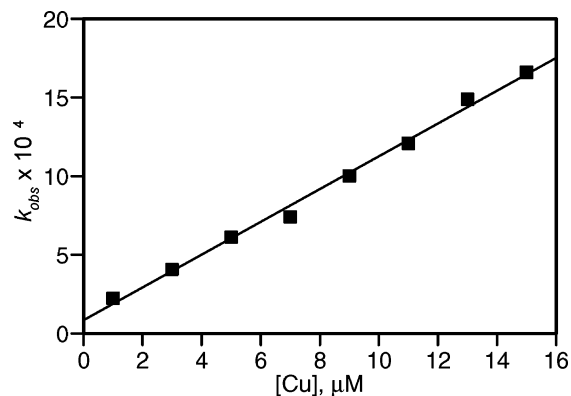


Figure 4. Observed rate constant (k_{obs}) vs $[\text{CuSO}_4]$ for the oxidation of $120\ \mu\text{M}$ H_2Asc , pH 4.5.

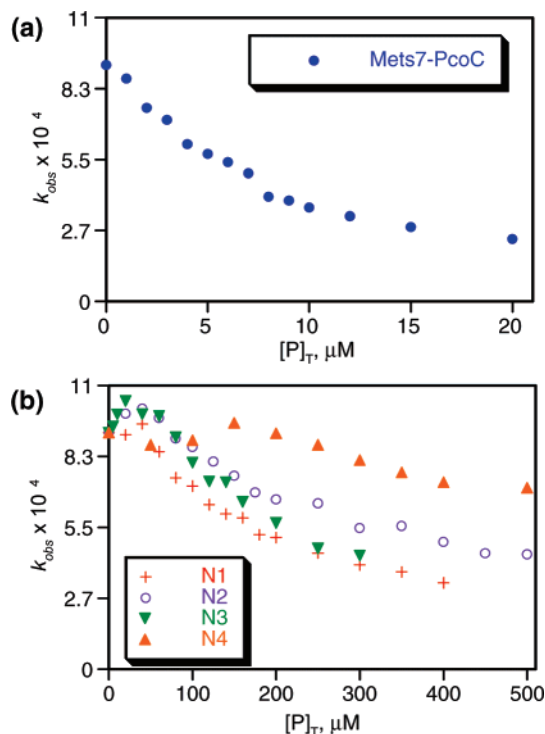


Figure 5. Plots of k_{obs} vs peptide concentration for the Cu-catalyzed oxidation of ascorbic acid ($120\ \mu\text{M}$ H_2Asc , $8\ \mu\text{M}$ CuSO_4). (a) **Mets7-PcoC** from 0 to $20\ \mu\text{M}$ dramatically decreases k_{obs} . (b) The effect of mutants **N1–N4** up to $500\ \mu\text{M}$.

slow the rate of ascorbate oxidation. This difference highlights the unique property of the $\text{MX}_2\text{MX}_2\text{M}$ motif of **Mets7-PcoC** in stabilizing reduced Cu(I). The mutants require significantly greater concentrations to achieve the same effect, suggesting that higher-order complexes are forming, not simple 1:1 adducts. The second major difference between panels a and b of Figure 5 is the increase in k_{obs} at low concentrations of **N1**, **N2**, **N3**, and **N4**. We observed a similar increase in k_{obs} for the amino acids methionine, *N*-acetylmethionine, and methionine methyl ester, as well as dimethyl sulfide (data not shown).

This increase in k_{obs} implies that inner-sphere electron transfer between HAsc^- and Cu(II) is favored in the presence of a monodentate thioether ligand. Rate acceleration has been previously observed in the anaerobic reaction of Cu(II) and ascorbate, where chloride increased the rate because of the

Table 4. Peptide Concentrations that Reduce k_{obs} by Half and the Effective K_{D} for Mets7-PcoC–Cu(I) Obtained from an Ascorbate UV Assay

peptide	$[P]_{\text{T}}$ at $1/2k_{\text{obs}}^a$ (μM)	K_{D} (μM)
Mets7-PcoC	7.5	2.5 ± 0.5
N1	240	
N2	450	
N3	265	
N4	1600	

^a In 8 μM Cu, 120 μM H₂Asc, pH 4.5.

favorable formation of CuCl.^{47,48} A species that complexes Cu(I) more strongly than Cu(II) will increase the rate of the redox reaction between Cu(II) and ascorbate, but will inhibit the catalytic reaction that occurs with O₂ or other oxidants.⁴⁷ In the case of peptides **N1**–**N4**, the soft thioether donor favors Cu(I), lowering the barrier for reducing Cu(II) to Cu(I). Without the chelating ability of multidentate **Mets7-PcoC**, however, Cu(I) can readily dissociate, reoxidize, and partake in catalysis. The rise in k_{obs} at low $[P]_{\text{T}}$ in Figure 5b therefore likely represents formation of the 1:1 PCu(I) complexes identified by mass spectrometry. At higher peptide concentrations, higher-order P_x:Cu ratios that stabilize Cu(I) and eventually slow catalysis are possible. We have not observed any P_{x>1}–Cu species by mass spectrometry, but this may be due to technical issues. Observation of P–Cu complexes of the mutant peptides requires conditions in which $[\text{Cu}] \gg [\text{pep}]$, disfavoring the binding of multiple peptides to one Cu.

As we do not know the P_x:Cu speciation, we have not used the ascorbate UV data to calculate effective K_{D} values for the mutants. Instead, we tabulate this information as the concentration of peptide required to reduce the copper-catalyzed oxidation rate of ascorbate by half. As shown by the values in Table 4, replacing even one methionine of **Mets7-PcoC** with a noncoordinating norleucine diminishes the peptide's ability to stabilize Cu(I) more than 30-fold for **N1** and **N3**, the mutants for which the Met residues are separated by two intervening amino acids. The effect is even more drastic when five intervening residues separate two Met residues, as the **N2** peptide is 60-fold less capable than **Mets7-PcoC** of slowing the copper-catalyzed ascorbate oxidation. Finally, the peptide that contains only one Met, **N4**, requires a concentration of more than 1.6 mM to have such an effect, a 200-fold difference.

The fact that metal chelators can decrease the rate of metal-catalyzed ascorbic acid oxidation has been known for some time. For many of the chelates studied, the decreased oxidation rate has been attributed not to the dissociation of the metal chelate followed by catalysis by free metal ion, but rather to the formation of mixed ligand chelates with HAsc[−] as a secondary ligand.⁴⁵ In this mechanism, the rate-limiting electron-transfer step between the metal and HAsc[−] depends on the stability of the metal chelate and the ability of HAsc[−] to coordinate the metal. Most of the chelates previously studied contain hard oxygen-rich donors that favor

higher oxidation states of Fe(III) or Cu(II), although the metal chelates are presumed to remain intact in both the reduced and oxidized forms throughout the catalytic cycle.⁴⁵

In the case of thioether-rich peptide **Mets7-PcoC**, however, the binding is dependent on the oxidation state being Cu(I), therefore formation of a [peptide–Cu(II)–HAsc[−]] ternary complex is unlikely. We favor a mechanism whereby **Mets7-PcoC** binds Cu(I) selectively, stabilizing it from reoxidation by O₂ and thereby removing it from the catalytic cycle. In our data analysis, we therefore assume it is unchelated, free Cu(II) ion that is responsible for HAsc[−] oxidation, not a PCu complex. Under this assumption, we can use the rate data to estimate an effective dissociation constant (K_{D}) for PCu(I). This value represents the concentration of free copper at which half of the peptide forms a peptide–copper complex under conditions of excess ascorbate to ensure the Cu(I) redox state. This method yields a K_{D} value of 2.5(5) μM for the 1:1 **Mets7-PcoC**–Cu complex, in excellent agreement with the value obtained from mass spectrometry.

To test the selectivity of **Mets7-PcoC** for Cu(I), we also investigated the influence of this peptide on iron-catalyzed ascorbate oxidation. To minimize hydrolysis of ferric iron, these studies were conducted at pH 1.75. We tested both EDTA and BCS, and found that each is capable of slowing the oxidation rate, verifying that even at this low pH, an Fe(III) chelator (EDTA) and an Fe(II) chelator (BCS) can attenuate the reaction. Addition of up to 30 μM **Mets7-PcoC**, however, had no effect on the iron-catalyzed reaction (data not shown). This result highlights the selectivity of **Mets7-PcoC** for Cu(I).

Discussion

Methionine-rich domains appear in several proteins involved in cellular copper trafficking, notably the high-affinity copper transporter Ctr1 as well as bacterial proteins PcoC, CopC, CusF, and bacterial Cu,Zn superoxide dismutase. By using two different methodologies, we have established that a peptide containing a distinctive MX₂MX₂M motif found in these proteins selectively binds Cu(I) with no detectable affinity for Cu(II). This is the first report that establishes an all-methionine environment for copper in biological systems.

The closest precedents for this unique binding mode are found in PcoC and CopC. EXAFS studies of PcoC are consistent with a three-coordinate Cu(I) site provided by two methionines and one N or O donor.¹⁹ The most likely location for this site is the Met-rich sequence MTGMKGMSHSPM spanning residues 41–53. A structure of apo-PcoC has been determined by X-ray crystallography;²⁰ the Met-rich region reproduced in Figure 6 showcases the Met and His residues that are candidate ligands. In the full structure, this region is a solvent-exposed loop that may be involved in protein–protein dimerization.²⁰ Our study on the simple peptide MTGMKGMS, which notably lacks one methionine and the histidine of the PcoC loop in Figure 6, substantiates the ability of a solvent-exposed loop to stabilize Cu(I) in a thioether-rich environment without having to bury the site within the protein. A very similar solvent-exposed loop in

(47) Xu, J.; Jordan, R. B. *Inorg. Chem.* **1990**, *29*, 2933–2936.

(48) Sisley, M. J.; Jordan, R. B. *J. Chem. Soc., Dalton Trans.* **1997**, 3883–3888.

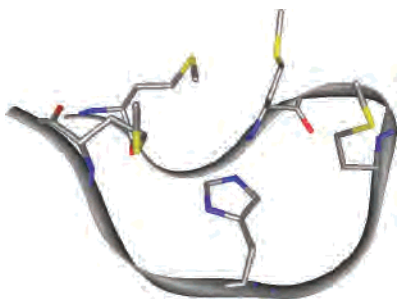


Figure 6. Structure of PcoC residues 41–53 (MTGMKGMSSHSPM), reproduced with coordinates from Protein Data Bank accession code 1LYQ. See ref 20.

CopC from *Pseudomonas syringae* has the sequence MTAMPGMEHSPM, and has been shown by EXAFS and NMR to bind Cu(I) with two or three S atoms and one His N atom.^{22,49} A K_D of 10^{-13} has been estimated for Cu(I) binding by the full-length CopC protein.²³ This binding affinity is significantly tighter than the value obtained here for the truncated peptide, which suggests that histidine may increase the affinity for Cu(I), or that the protein architecture pre-organizes the loop to create a macrocyclic effect for chelation, as suggested by the NMR structure.²²

In addition to a novel binding mode, the current studies also provide chemical evidence to support the hypothesis that Ctr1 transports Cu(I). Because Cu(I) can react with H_2O_2 to form hydroxyl radicals, it is the more dangerous copper oxidation state for a cell. However, the fact that it is more exchange labile than Cu(II) facilitates its transfer between two binding sites, making it chemically reasonable that proteins involved in copper trafficking favor Cu(I). The challenge for these sites is then to provide an environment that can safely sequester Cu(I) in an oxidizing environment like the extracellular space. The methionine-rich N-terminus of Ctr1 provides such a coordination environment. Polythiaether macrocycles have been shown to significantly increase the Cu(II)/Cu(I) redox potential compared with polyaminothiaether or polyamine macrocycles.^{50,51} These complexes are good models of the binding sites found in Mets motifs, in which an all-methionine binding site likely increases the redox barrier in order to stabilize Cu(I) at the plasma membrane and prepare it for transport into the cell.

We have calculated the effective dissociation constant for the 1:1 complex between the **Mets7-PcoC** peptide and Cu(I) by two independent methods that both utilize ascorbic acid to generate Cu(I) and provide an effective K_D value of $\sim 2.5 \mu M$ at pH 3.5–4.5. These results show that individual, discrete Mets domains are sufficient for binding Cu(I) with low micromolar affinity, establishing the lower end of how such motifs might bind Cu(I) in the context of the full protein. We do not yet know whether the affinity would be tighter in the full-length construct. Given that the K_M values

for Ctr1-mediated copper transport have been reported to be between 1 and $5 \mu M$ in a variety of organisms,⁶ a tighter binding site might not be advantageous to the function of the extracellular Mets domains of Ctr1.

Furthermore, these results suggest that protein oligomerization is not obligatory for the copper acquisition function of Mets motifs. Several studies indicate that Ctr1 oligomerization is required for transport of Cu through the membrane.¹³ Mutation studies in yeast have revealed that although Mets motifs are necessary for growth under low copper conditions, they are not essential for copper transport when copper is plentiful,^{8,9} and therefore they are not likely to be part of the actual transmembrane transport mechanism. We therefore favor the hypothesis that Ctr1 performs at least two independent functions: extracellular copper acquisition and transmembrane copper transport. A third function would be copper transfer to intracellular chaperone proteins.¹⁴

The results here imply that individual Mets motifs can perform the function of copper acquisition with an affinity commensurate with biological copper uptake. The second function of trans-membrane transport is more complicated. All Ctr1 proteins possess an MXXXM motif in the second transmembrane domain that, unlike the Mets motifs, is essential for copper transport.⁹ Our results from the norleucine mutant peptides indicate that three methionine residues are required for biologically reasonable 1:1 binding with Cu(I). Two methionine residues separated by two intervening residues still accommodate Cu(I), but with much diminished affinity, and separating the two methionines even further, such as in peptide **N2**, further weakens binding. We speculate that an unstructured MXXXM alone is not sufficient for copper binding, and suggest that these transmembrane regions may form a Met-rich channel formed via protein oligomerization. In this scenario, the extracellular Mets domains acquire, stabilize, and concentrate Cu(I), perhaps acting as a selectivity filter, to pass it through a thioether channel in the membrane. Others have suggested similar scenarios.^{9,17}

An alternative pathway for copper homeostasis has been uncovered that involves copper-dependent endocytosis and degradation of Ctr1.^{16,17} Although not likely to be the primary mechanism of action of Ctr1, it may be a complementary or situation-specific route. Under conditions that favor this pathway, the Mets domain closest to the first transmembrane region of hCtr1 is required for copper-stimulated endocytosis at low copper levels.^{16,52} These results beg the question of whether Cu(I) binding to a specific Mets domain may play an additional, copper-sensing role that instigates an endocytosis pathway. Uncovering the coordination chemistry of these specific Mets domains will be an important step in understanding copper homeostasis.

Acknowledgment. We thank Prof. Dennis J. Thiele and Erin M. Rees for many helpful discussions, and Duke University for funding.

IC051180M

(49) Arnesano, F.; Banci, L.; Bertini, I.; Thompsett, A. R. *Structure* **2002**, *10*, 1337–1347.

(50) Dockal, E. R.; Jones, T. E.; Sokol, W. F.; Engerer, R. J.; Rorabacher, D. B. *J. Am. Chem. Soc.* **1976**, *98*, 4322–4324.

(51) Rorabacher, D. B. *Chem. Rev.* **2004**, *104*, 651–697.

(52) Ooi, C. E.; Rabinovich, E.; Dancis, A.; Bonifacino, J. S.; Klausner, R. D. *EMBO J.* **1996**, *15*, 3515–3523.